THEORETICAL SIMULATION OF CURE-INDUCED DEFORMATIONS OF COMPOSITE CAR BODY PANELS

M. S. Kiasat [*], *H. Mostofi* [†]
[*]*Department of Marine Tech., Amirkabir University of Technology, Tehran, Iran*
kiasat@aut.ac.ir

[†]*Department of Automotive Eng., Iran University of Science and Tech., Iran*
hamid7961@yahoo.com

Abstract

This paper is dedicated to a realistic prediction of the deformations of advanced composite car body panels during curing. In the present work, a cure-dependent viscoelastic model is used for the resin to establish the cure-dependent orthotropic viscoelastic properties of a unidirectional glass/polyester ply via micromechanical fiber/matrix models. Also, the anisotropic curing shrinkage of the unidirectional ply is obtained from unit cell calculations by inserting the measured curing shrinkage of the resin. These evaluated properties are used in the finite element model of the laminate which is verified by an experimental study of the deformations of square cross-ply laminates. As an application of this effort, different parts of a car body like the roof and the trunk are modeled considering various symmetric and asymmetric stacking sequences for them. Both open-mold and closed-mold curing conditions are simulated. It is concluded that the curing stresses have a viscoelastic nature which may not be modeled by using the available elastic models. The curing stresses induce significant deformations in the composite panels which cannot be avoided even if symmetric laminates are cured in closed molds. The initial curvatures and bends of the panel in the mold affect its final deformed shape.

Introduction and Overview of Literature

The importance of the shrinkage effects in the composites is the main reason to study the curing process of the thermosets. The magnitude of the curing stresses depends on various parameters such as the fiber volume fraction, and it should be noted that these stresses may become quite substantial. Shrinkage of the matrix of a composite may have three important consequences; the warpage of the product due to the anisotropic shrinkage of different layers, sink marks at the surface causing a reduced appearance of the product, and the material micro-cracking damage resulting in reduced strength properties.

Warpage in composite products is a frequent concern during manufacturing. It is directly related to the residual stresses, which may arise due to resin shrinkage during curing and cooling. The development process of the residual stresses during curing, and the simultaneous viscoelastic stress relaxation are still not completely investigated. There are relatively few works on modeling the varying time-dependent behavior of a curing thermoset resin. This is mainly due to the difficulties concerning the mechanical characterization of the material during curing. In the early treatments of the processing, the stress arising from the chemical curing shrinkage was acknowledged, but was not addressed because of its complexity. Some authors later proposed that the curing residual stresses (before cool down) are not significant [1]. They reasoned that since the curing shrinkage occurs at early curing stages, where the resin is in the rubbery state, there is sufficient time for any curing stress to relax before cool down. The invalidity of this assumption was shown by Kiasat *et al.* [2] where quite significant curing stresses were measured in resin specimens subjected to dimensional constraints before cool down. The modeling of the thermally-induced warpage of short fiber composites has been studied by Tseng *et al.* [3]. They used a cure-dependent elastic model for the resin to decrease the complexity of the process by ignoring relaxation.

To develop a viscoelastic model for the curing resin, it has been common to consider the effect of the "progress in curing" as that of the "decrease in temperature" [1,4]. On this basis, the relaxation times of the material have been assumed to increase with the degree of cure. In other words, the material has been assumed to obey an equivalent time-temperature superposition for the curing. This behavior has never been observed experimentally. Wiersma *et al.* [5] investigated the change of the configuration of L-shaped composite parts after releasing from the mould and cooling to ambient temperature. They found that the decrease of the angle of such parts, called springforward phenomenon, cannot be completely predicted from the anisotropic thermal shrinkage of the lamina due to cooling from the curing temperature. Hyer [6] investigated the dependency of the curvature upon the side length of asymmetric cross-ply laminates having different thicknesses. He obtained a reasonable modeling of the laminate deformations by using nonlinear strain-displacement relations. Capehart *et al.* [7] simulated the deformation of composite car body panels after curing and removing from the mould. They did not consider the viscoelastic behavior of the composite.

In the present work, a newly developed and verified cure-dependent viscoelastic model [8] for the mechanical behavior of the polyester resin in an isothermal curing reaction (in thin layers) is used to establish the cure-dependent orthotropic viscoelastic properties of the unidirectional glass/polyester lamina. The calculated curing properties of the lamina are applied in the finite element modeling of the laminates. Due to the large deformation of the laminates, nonlinear strain-displacement equations are used in the finite element modeling, which leads to comparable results. The resin formulation in this research is chosen so that its curing process at 70°C completes for about 5 hours. This slow curing reaction enabled us to perform dynamic mechanical tests at high and low frequencies on the resin during curing which are required for our modeling. In industry, composite car body panels are manufactured with rather high-rate curing processes at higher temperatures. For gathering material data in such cases, dynamic excitations must only be applied at high frequencies. Thus the procedure described in this paper is still applicable to such high-rate curing processes, as asked by the respected reviewer, and also our viscoelastic model can take the simultaneous stress relaxation into account.

Cure-Dependent Viscoelastic Model for Resin

The solidification of a thermosetting resin results from a chemical curing reaction. The characteristics of the resin change from the behavior of a viscoelastic liquid with a low shear stiffness in the uncured state, to the behavior of a viscoelastic solid with a relatively high stiffness in the fully cured state. The relaxation moduli of the curing resin, like the relaxation Young's modulus and the relaxation shear modulus, are thus functions of not only the time t but also the degree of cure α. The relaxation Young's modulus $E(\alpha,t)$ of the resin at various degrees of cure is schematically shown in Figure 1. The relaxation modulus at a degree of cure α may be different in the shape and the level with that at a higher α. If such data are available for the characteristic function of the resin, then the normal stress component $\sigma(t)$ at current time t which is induced due to the application of a varying extensional strain $\varepsilon(\zeta)$ during a curing process is determined as

$$\sigma(t) = \int_{-\infty}^{t} E\big(\alpha, t-\zeta\big)\frac{d\varepsilon(\zeta)}{d\zeta}\,d\zeta \tag{1}$$

Equation (1) is based on Boltzmann superposition principle for the linear viscoelastic materials, in which the cure dependency of the relaxation modulus is taken into account. The data for the cure-dependent relaxation modulus over some specified time decades can be fitted by an exponential series having enough number of terms N, and only cure-dependent intensities $E_n(\alpha)$ for each term, see Eq. (2).

$$E(\alpha,t) = \sum_{n=1}^{N} E_n(\alpha)\,\exp\!\left(-\frac{t}{\tau_n}\right) \tag{2}$$

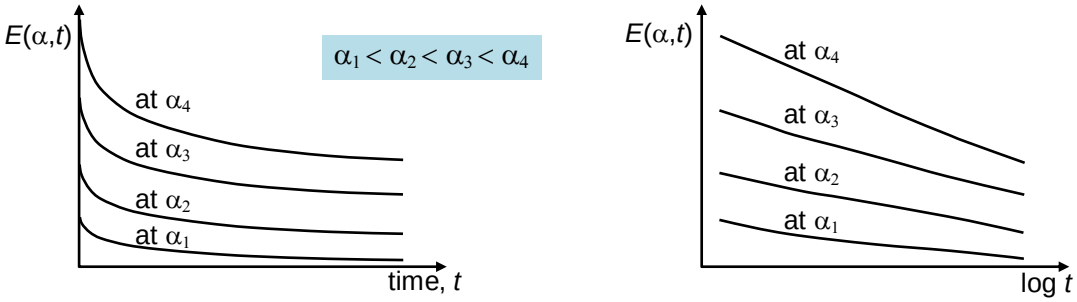

Figure 1: Schematically shown relaxation Young's modulus E(α,t) of the curing resin.

Such an exponential series may have one or two relaxation times τ_n in each time decade. The components of the relaxation function tensor C_{ij} for the isotropic resin are combinations of the cure-dependent relaxation shear and bulk moduli, as below

$$C_{ij}(\alpha,t) = G(\alpha,t)\, D_{ij} + K(\alpha,t)\, V_{ij} \qquad (i,j = 1,...,6) \tag{3}$$

where the relaxation shear modulus $G(\alpha,t)$ and the relaxation bulk modulus $K(\alpha,t)$ are described by exponential series like in Eq. (2), and D_{ij} and V_{ij} are the components of the deviatoric and volumetric constant matrices, respectively. The constitutive relation, for the curing material, between the components of the stress tensor σ_i at the current time t and the components of the strain tensor ε_j applied at any time ζ is described like in Eq.(1), as below

$$\sigma_i(t) = \int_{-\infty}^{t} C_{ij}(\alpha, t-\zeta)\frac{d\varepsilon_j(\zeta)}{d\zeta}\, d\zeta \qquad (i,j = 1,...,6) \tag{4}$$

In this work, the data for the relaxation moduli is indirectly gathered through dynamic mechanical analysis (DMA) of the resin during curing. DMA tests are performed by applying two types of deformation separately, i.e. shear and longitudinal bulk deformations, which result in the data for the storage moduli $G'(\alpha,\omega)$ and $K'(\alpha,\omega)$ as functions of the frequency ω and α. This data for the storage moduli is fitted by fractional series (5) in frequency domain, which corresponds Eq. (2) in time domain, and the cure-dependent $G_n(\alpha)$ are calculated while the relaxation times τ_n are chosen within considered decades. The parameters $K_n(\alpha)$ are similarly calculated [8].

$$G'(\alpha,\omega) = \sum_{n=1}^{N} G_n(\alpha)\frac{(\omega\tau_n)^2}{1+(\omega\tau_n)^2} \tag{5}$$

The constitutive equation (4) may be used for anisotropic curing material as well, where the functions $C_{ij}(\alpha,t)$ are not anymore combinations of G and K as in Eq. (3), but are separately described by exponential series like in Eq. (2) using $C_{ij}^n(\alpha)$, see Eq. (6)

$$C_{ij}(\alpha,t) = \sum_{n=1}^{N} C_{ij}^n(\alpha)\, \exp\left(-\frac{t}{\tau_n}\right) \tag{6}$$

Incremental Constitutive Equation

Regarding the complexity of the material cure-dependent relaxation functions and the curing shrinkage strain, the above constitutive equation cannot be solved analytically even in a one-dimensional problem. Therefore, the integral constitutive equation is converted into an incremental one within time steps, which can properly be used in the finite element method. To develop the incremental stress-strain relation, the relaxation function tensor is substituted in the integral equation (4), and the total time interval is divided into a number of subintervals $[t_{m-1}, t_m]$ with a time step of $h = t_m - t_{m-1}$. Therefore, the increment of the total stress is related to the increment of the strain as

$$\Delta\sigma_i(t_m) = \left\{\sum_{n=1}^{N}\frac{\tau_n}{h}[1-\exp(\frac{-h}{\tau_n})]C_{ij}^n(\alpha_{m-1/2})\right\}\left[\Delta\varepsilon_j(t_m) - \Delta\varepsilon_j^0(t_m)\right] + \sum_{n=1}^{N}\left[\exp(\frac{-h}{\tau_n})-1\right]\sigma_i^n(t_{m-1}) \tag{7}$$

Equation (7) is an “incremental stress-strain relation” which is here obtained for the general anisotropic cure-dependent viscoelastic material. In this equation, the current increment of stress is equal to a factor of the current increment of strain, plus a term containing the stress in the previous time step. Therefore, the stress-strain relation changes with the curing time, and the finite element stiffness matrices must be recalculated in each time step. The curing shrinkage of the resin is treated as an initial strain which is incrementally applied at the beginning of each time step $\Delta\varepsilon_j^0(t_m)$. Obviously, the shear components of this initial strain increment are zero.

Orthotropic Properties of a Unidirectional Ply

In order to model the cure-induced deformation of a composite laminate, orthotropic viscoelastic properties of its constituting unidirectional laminas are required. The transverse properties of the lamina (perpendicular to the fiber direction) depend not only on the properties of the matrix and the fibers but also on the transverse distribution of fibers in the matrix. Different models are proposed in literature to combine the elastic properties of the matrix and the fibers to obtain the lamina properties, e.g. by Halpin-Tsai. However, when time-dependent properties are to be taken into account, these models are not recommended. In the present work, a hexagonal transverse distribution is assumed for the fibers, see Figure 2(a). This can lead to realistic results when a moderate fiber volume fraction v_f of 0.5 is considered. The difference of various micromechanical models increases with the fiber volume fraction. The hexagonal fiber-arrangement is preferred to the square fiber-arrangement because of the lack of transverse isotropy for the square arrangement.

A planar unit cell is discretized into planar finite elements with a generalized plane-strain formulation, Figure 2(a). In order to obtain the relaxation moduli and Poisson’s ratios of the lamina at a degree of cure, the relaxation moduli of the resin at that degree of cure are used for the matrix. Elastic properties of E-glass fiber are also applied. A step constant tensile strain of 1% is then applied in X direction and kept constant, and the relaxation of stress in X direction is studied. This deformation is applied to obtain the transverse Young’s modulus $E_T(\alpha,t)$ the transverse-transverse Poisson’s ratio $\nu_{TT}(\alpha,t)$, and the transverse-longitudinal Poisson’s ratio $\nu_{TL}(\alpha,t)$, of the lamina. Time-dependent calculations are performed at some various degrees of cure. The time steps in each calculation are given over more than 6 time decades corresponding to five hours curing time. Figure 2(b) shows the distribution of the stress in X direction over the vertical right side of the cell. The response of the cell is obtained by integrating this stress over the side of the cell at any time within the considered time decades divided by the side area.

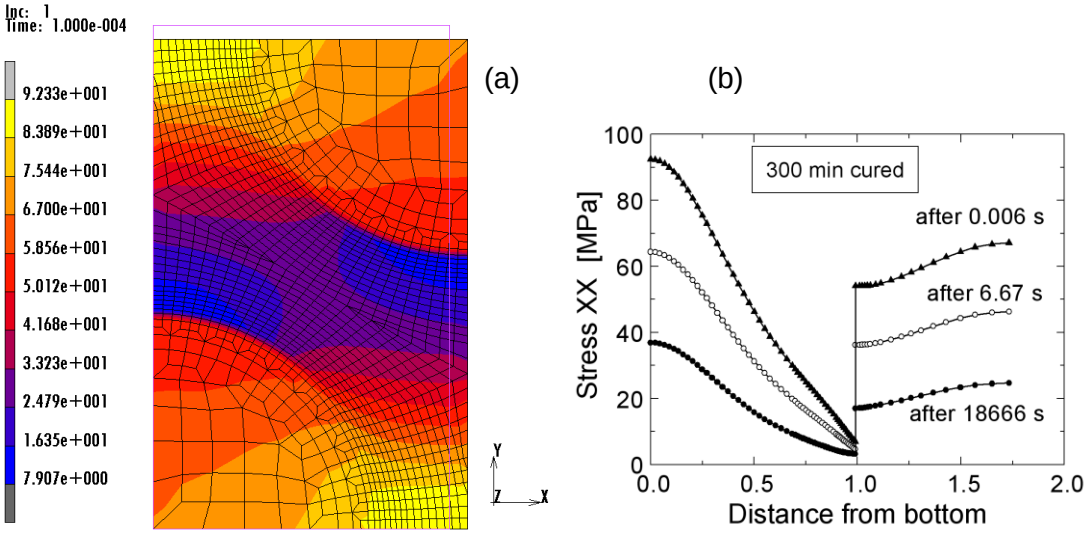

Figure 2: Distribution of stress XX at a short time (0.0001 min) after the application of 1% tensile strain in X direction at 300 min curing, (a) on unit cell, (b) on right edge.

Such calculations are repeated at different degrees of cure. The results are shown in Figure 3(a) where the transverse modulus $E_T(\alpha,t)$ of the lamina is obtained by dividing the responded stress by the applied constant global strain. It is observed that the transverse modulus of the lamina is strongly cure- and time-dependent. This is expected since the mechanical behavior of the matrix is predominant in transverse direction. In order to use the transverse modulus in the laminate calculations, the data in Figure 3(a) is fitted by an exponential series like in Eq. (2) with eight terms. The relaxation times τ_n are chosen logarithmically equally spaced over 6 time decades, see Table I. The cure-dependent coefficients of the exponential terms $E_{Tn}(\alpha)$ are then obtained through the fitting process for any degree of cure , Figure 3(b). Since the modulus has a linear-like behavior with the logarithm of the time, the coefficients E_{T1} to E_{T7} are taken equal.

The transverse-transverse Poisson's ratio, $\nu_{TT}(\alpha,t)$ is obtained when dividing the time-dependent displacement of the upper side of the unit cell by the initial length of the cell in Y direction, and then dividing it by the constant strain applied in X direction with a negative sign. The results are shown in Figure 3(c) at four various degrees of cure. It is observed that the transverse-transverse Poisson's ratio $\nu_{TT}(\alpha,t)$ increases during the relaxation of the transversal stresses. This is because of the mechanical behavior of the matrix resin. At low degrees of cure, $\nu_{TT}(\alpha,t)$ is about unity and it decreases towards about 0.47 with the increase of the degree of cure.

The transverse-longitudinal Poisson's ratio, $\nu_{TL}(\alpha,t)$, of the lamina is obtained from the calculated strain in the fiber direction, perpendicular to the planar unit cell, which is responded to the strain applied in X direction. The results are shown in Figure 3(d). It is observed that the contraction in the fiber direction due to tension in the transverse direction is several order of magnitude less than the contraction in the other transverse direction, compare Figures 3(c) and 3(d). Further, the transverse-longitudinal Poisson's ratio decreases during the relaxation of the transverse stresses. This is due to the elastic behavior of stiff fibers which gradually elongate after their initial contraction.

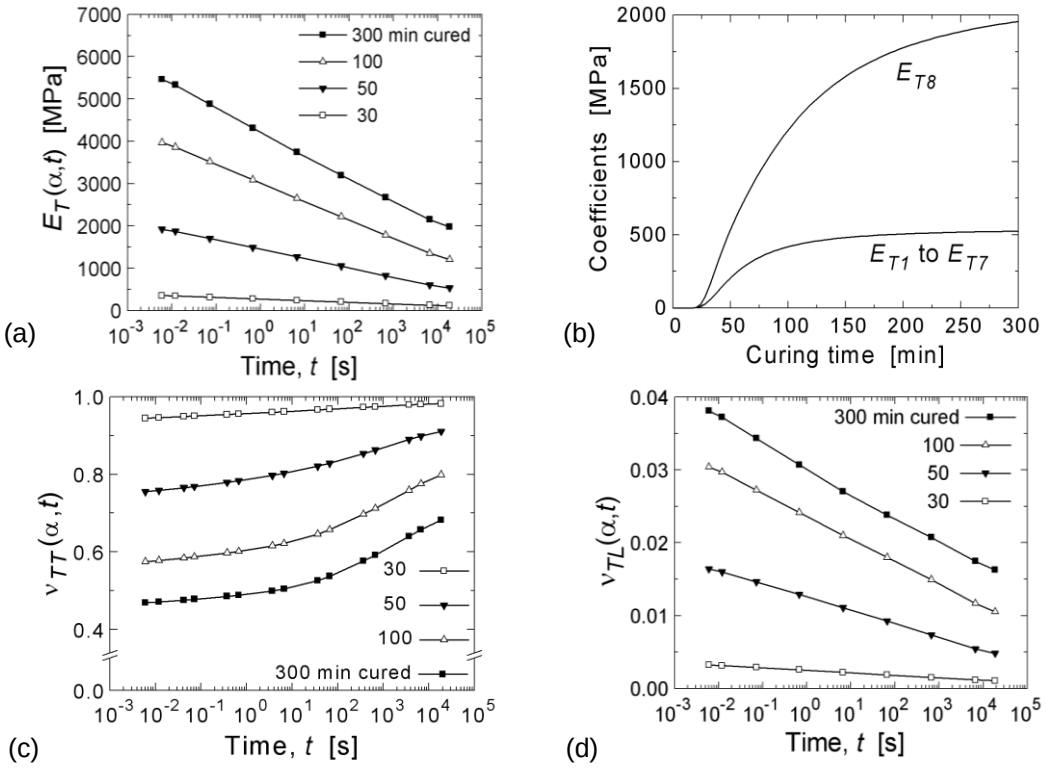

Figure 3: (a) Transverse modulus of a unidirectional ply, (b) coefficients of fitted exponential series, (c) transverse-transverse Poisson's ratio of a ply, and (d) transverse-longitudinal Poisson's ratio of a ply.

Table I: Relaxation times for the exponential series

n	1	2	3	4	5	6	7	8
τ_n [s]	0.0167	0.1415	1.2019	10.206	86.670	735.99	6250	∞

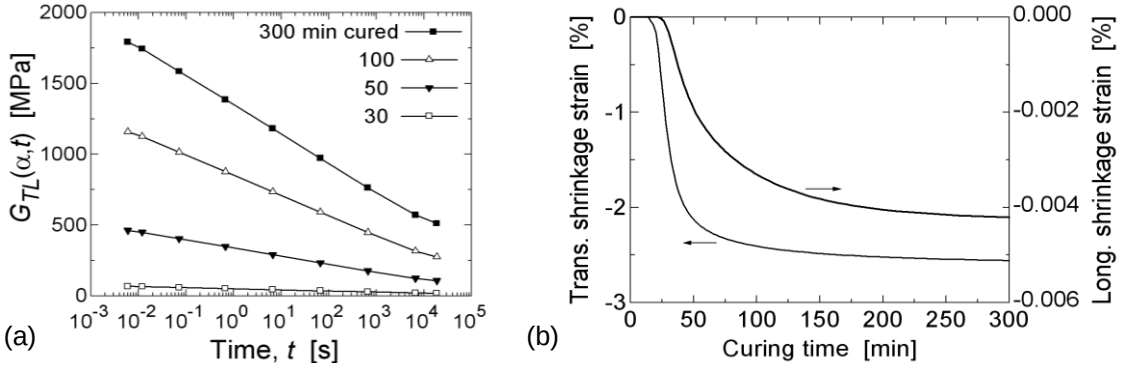

Figure 4: (a) Transverse-longitudinal shear modulus, (b) Transverse and longitudinal curing shrinkage strain of a lamina with a fiber volume fraction of 0.5.

The transverse-longitudinal shear modulus $G_{TL}(\alpha,t)$, as another independent property of the lamina, is obtained by applying a shear deformation on a 3-D unit cell of the hexagonal fiber-arrangement. The stresses responded by the unit cell of the lamina decrease with time although the global shear strain is kept constant. The relaxation shear modulus $G_{TL}(\alpha,t)$ is obtained when integrating the shear stress over the side of the unit cell and dividing that by the side area and applied global shear strain at each time step, see Figure 4(a). The longitudinal Young's modulus $E_L(\alpha,t)$ and the longitudinal-transverse Poisson's ratio $\nu_{LT}(\alpha,t)$ of the lamina can readily be calculated by using the rule of mixture as

$$E_L(\alpha,t)=v_f E_f + v_m E_m(\alpha,t) \tag{8}$$

for the longitudinal modulus. It is observed that the relaxation in the fiber direction is at most about 2% during five hours, which is expected due to the elastic stiff fibers. All cure-dependent properties of lamina are fitted by exponential series as done for the transverse modulus.

Orthotropic Curing Shrinkage of a Ply

The shrinkage of a lamina is due to the curing shrinkage of its thermosetting matrix. In order to determine the shrinkage of the lamina in different directions, a unit cell analysis is performed in which the sides of the unit cell, made up of generalized plane-strain elements, are left free to move parallel to each other when the matrix shrinks. The curing shrinkage of the resin is measured in a newly designed setup [2]. Different fiber arrangements are considered here. It is observed that the shrinkage strain of the lamina is not dependent on fiber arrangement, but well dependent on the fiber volume fraction. The shrinkage strain in the transverse and longitudinal directions obtained from the unit cell calculations for a fiber volume fraction of 0.5 is shown in Figure 4(b).

Experimental Study of Cure-Induced Warpage

Cure-induced deformations of asymmetric cross-ply [0/90] laminates are experimentally studied in the present work. The cross-ply laminates are designed with a thickness of about 1 mm and the fiber volume fraction of about or less than 0.5 to obtain significantly curved panels. The cross-ply laminates are made up of a commercial E-glass fabric which is composed of two unidirectional arrays of fiber bundles aligned in perpendicular directions and knitted together with thin polyester threads. The fabric is cut in a square shape with a side length of about 240 mm, and it is impregnated with the liquid unsaturated polyester resin. Release-agent-treated plastic sheets are used to prevent the adhesion of the laminate to the heated mould.

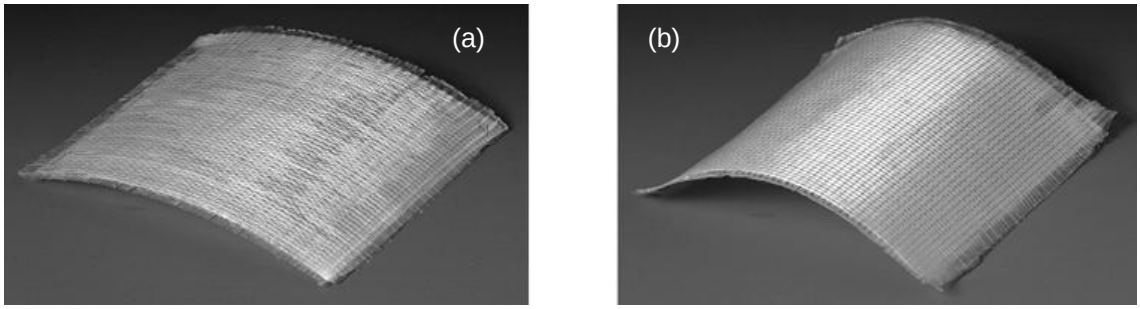

Figure 5: (a) Glass/polyester [90/0] laminate cured between aluminum plates for five hours and then released, (b) a similar laminate freely cured for five hours.

Providing suitable uniform and constant heat transfer conditions at both sides of the laminate is very important. This is because the temperature changes and nonuniformity of the curing are not taken into account in the model. Such modeling is relevant for most of the thin laminates produced in industry. Uniform heat transfer condition is simply provided by curing the laminates between two identical aluminum plates. It is observed that the laminates take a cylindrical shape after releasing from the aluminum plates at the end of the five-hour curing, Figure 5(a). A cylindrical shape, instead of a saddle shape, is expected because of the large length-to-thickness ratio of the produced laminates [6].

Another curing method is also applied in the present work to study free deformations of laminates during curing. To provide a uniform heat transfer condition at both laminate sides, uncured laminates are laid on a honeycomb foam layer in an air-circulation oven, over which another foam layer is placed at a distance of about 7 cm. Figure 5(b) shows a laminate that is freely cured and become cylindrical. It is observed that the curvature of the freely cured laminates is more than that of the laminates which are cured between aluminum plates. This is attributed to the partial relaxation of the curing stresses in the laminates which are constrained between aluminum plates. The severe curvatures experimentally observed here are just due to the curing shrinkage of the resin, before the occurrence of any thermal shrinkage due to cool down.

Table II shows the experimental results for five laminates having different thicknesses and matrix volume fractions, v_m. These laminates were cured between aluminum plates. The matrix volume fraction of the laminates, determined by examining some pieces of the laminates, increases with the thickness of the laminates since almost the same reinforcing fabric is used in the laminates. The increase of these two laminate specifications, i.e. v_m and thickness, will affect the curvature of the laminate in contrary ways. The higher the v_m the higher the curvature (at a constant thickness), which is because of the increase of the shrinkage of the plies in transverse direction. On the other hand, the thicker the laminate the lower the curvature (at a constant v_m), which is due to the higher area moment of inertia of the laminate. It is observed that from Laminate 1 to Laminate 3 the curvature increases (radius decreases) due to the increase of the matrix volume fraction which is therefore more affective than the thickness. However, Laminates 4 and 5 have lower curvatures (larger radii) which is due to the more significant increase of the thickness relative to the v_m.

Table II: Specifications of Laminates cured between two aluminum plates and released at the end of curing.

	Thickness [mm]	Average v_m	*Radius of curvature* [mm]
Laminate 1	0.80	0.50	373
Laminate 2	0.95	0.60	288
Laminate 3	1.00	0.70	176
Laminate 4	1.20	0.75	301
Laminate 5	1.40	0.80	263

Modeling Cure Deformations of Square Laminates

Quadrilateral 8-node thick shell elements are used for the finite element modeling of a square laminate 240 mm in length and 0.8 mm in thickness, with a matrix volume fraction of 0.5. The effects of through- thickness shear deformations are taken into account for such an element. Further, the geometrical nonlinearity is considered since the deflection of the laminate is many times its thickness. The laminate is simply supported at its corners. The calculated viscoelastic properties and anisotropic curing shrinkage are applied for the lower lamina (in Y direction) and the upper lamina (in X direction) of the laminate.

Figures 6(a) and 6(b) present a comparison between the results of the geometrically linear and nonlinear finite element analyses. The figure shows the deformed shape and also the outline of undeformed shape of a laminate at the end of the 300-min curing which is cured freely. It is observed that when the geometrical nonlinearity is not taken into account the laminate is predicted to develop a saddle shape (anticlastic shape) with different curvatures in X and Y directions, Figure 6(a). However, with geometrical nonlinearity, a cylindrical shape is predicted, Figure 6(b), which agrees the experimental observations, Figure 5(b). In the case of large laminates, the formation of the curvature in one direction prevents the formation of the curvature in the other direction due to the increase of the area moment of inertia of the cross section.

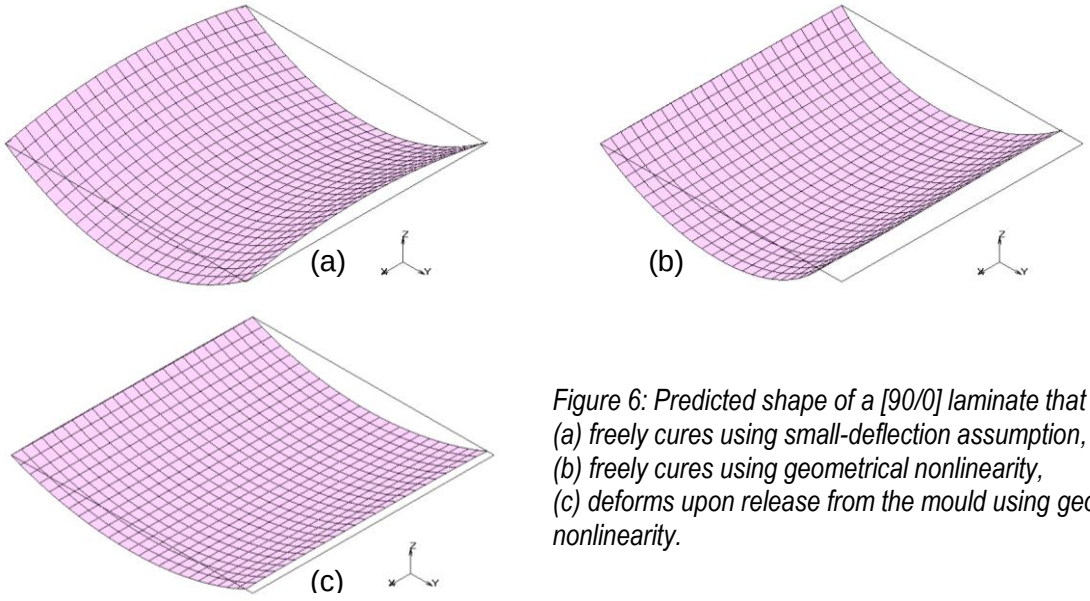

Figure 6: Predicted shape of a [90/0] laminate that
(a) freely cures using small-deflection assumption,
(b) freely cures using geometrical nonlinearity,
(c) deforms upon release from the mould using geometrical nonlinearity.

The other modeling to be presented here is for a laminate which cures between two aluminum plates. In this case, all nodes in the mesh are given zero displacement for 300 minutes curing, and then they are released within few seconds. The deformation of the laminate at the end of the analysis is shown in Figure 6(c). Figure 7 presents the development of the radius of cylindrical curvature of the asymmetric laminate during curing. The curvature is calculated from the vertical displacement (in Z direction) of the midpoint of the laminate and the horizontal displacement (in Y direction) of its free edge. A significant difference is obtained between the curvature of the freely cured laminate and that of the laminate released at the end of the curing. Such a difference is also observed in our experimental study, Figure 5. This proves that our cure-dependent viscoelastic model is able to realistically predict the deformations of the curing laminates. It is noted that when using cure-dependent elastic models [3,7], such an experimentally observed difference of curvatures can never be predicted.

Figure 7 shows that the predicted radius of curvature of the laminate which cures in the mold and then released is comparable with the experimental result presented in Table II for Laminate 1 having the same thickness and v_m as in our modeling.

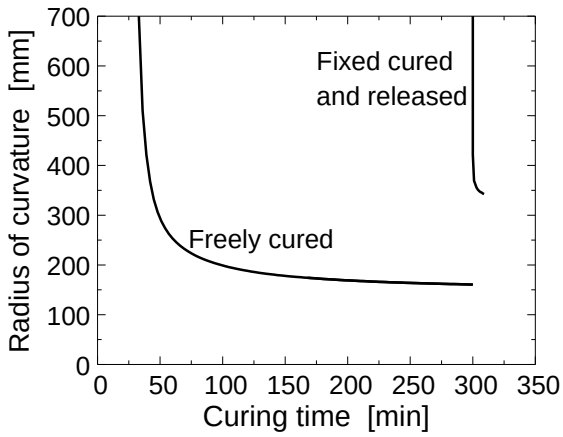

Figure 7: Results of modeling for the development of the radius of cylindrical curvature of [90/0] laminates.

Predicting Cure Deformations of Car Panels

The finite element models of a number of car body panels are constructed and analyzed in this investigation. The analysis of a trunk and a roof are presented in this section. The model of the trunk is shown in Figure 8(a). Shell elements with the same specifications as in the previous section, and geometrical nonlinearity for large deformations are used. Two different glass/polyester laminates with the same thicknesses of 1 mm are applied for this panel; an asymmetric [0/90] laminate, and a symmetric [0/90/90/0] laminate. The viscoelastic properties and the curing shrinkage of the laminas during five-hour curing are those calculated in the previous sections. Simple support boundary conditions are used to prevent rigid body motions, and thus the curing is assumed to be done in an open mould.

The results of the nonlinear analyses are presented in Figures 8(b) and 9. Severe deformation of the asymmetric laminate, Figure 9, shows the strong effect of the curing stresses on the L shape of the trunk. This deformation is completely asymmetric and quite different from the cylindrical shape experimentally observed for the square laminates in Figure 5(b). In the case of the freely cured symmetric laminate, Figure 8(b), the deformation of the trunk is symmetric but it is still very significant. The L shape of the trunk is somewhat opened (shown by the arrow) and a significant concavity is observable on the vertical part of the trunk. Figures 10(a) and 10(b) present the deformation of the symmetric-laminated trunk quantitatively. It is observed that the displacement in X direction of a node at the bottom corner of the trunk starts increasing rapidly at the gel time of the resin. The displacement of this node increases up to 28 mm and afterwards it decreases and gradually flattens. The decrease of the displacement of this node is due to the displacements of the other nodes of the trunk which has a complex deformation during curing.

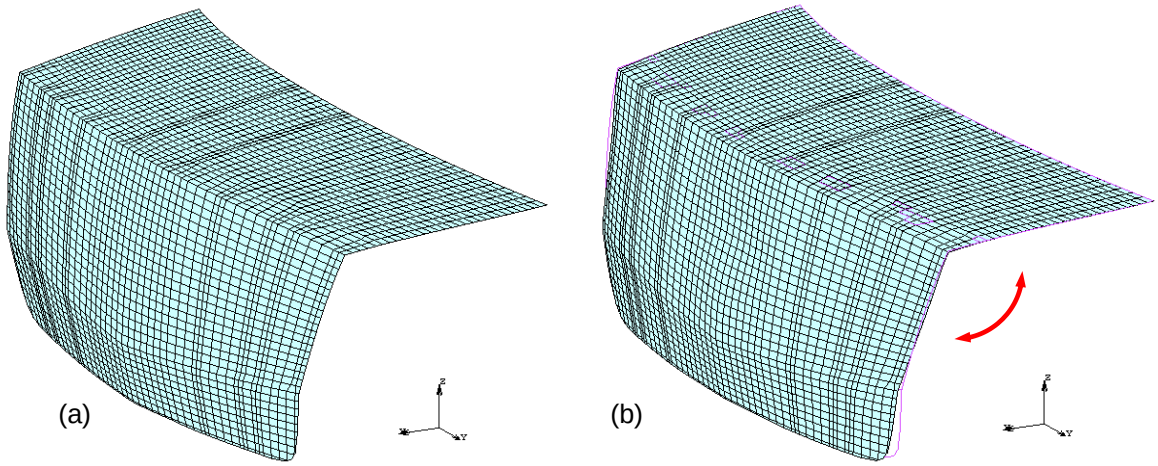

Figure 8: (a) Finite element model of a composite trunk, (b) deformed shape of an open mould (freely cured) symmetrically-laminated trunk at the end of the curing.

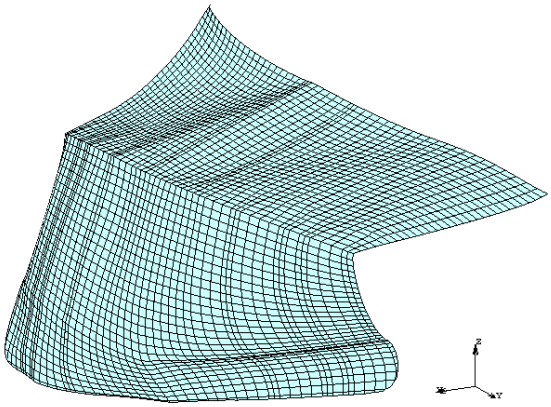

Figure 9: Deformed shape of an open mould (freely cured) asymmetrically-laminated trunk at the end of the curing.

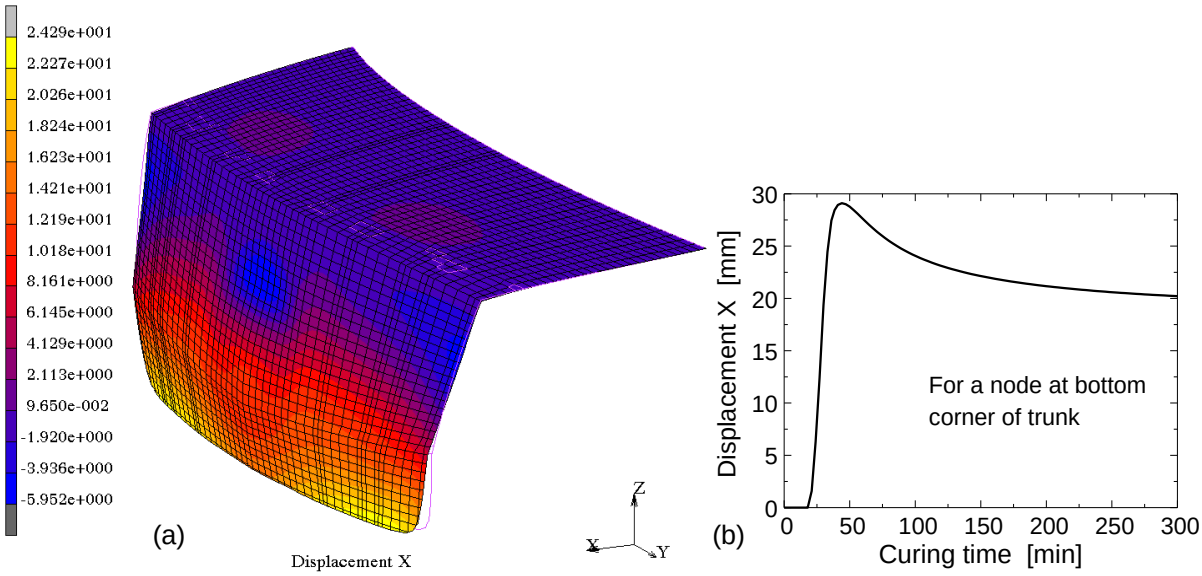

Figure 10: (a) Distribution of displacement in X direction at the end of the curing, (b) Development of displacement at a node at the bottom corner of the trunk.

The finite element model for the roof is shown in Figure 11. A symmetric [0/90/90/0] glass/polyester laminate with a thickness of 1 mm is applied for this panel. The viscoelastic properties and the curing shrinkage of the laminas are those calculated in the previous sections. Two different curing conditions are applied for the analysis of the roof; free curing condition (open mould) and constrained curing condition (closed mould). For the free curing condition, only simple support boundary conditions are used to prevent rigid body motions, see Figure 11. For the closed mould condition, all nodes in the mesh are given zero displacement for five hours curing, and then they are released within few seconds. The results of the nonlinear analyses are shown in Figures 12(a) and 12(b).

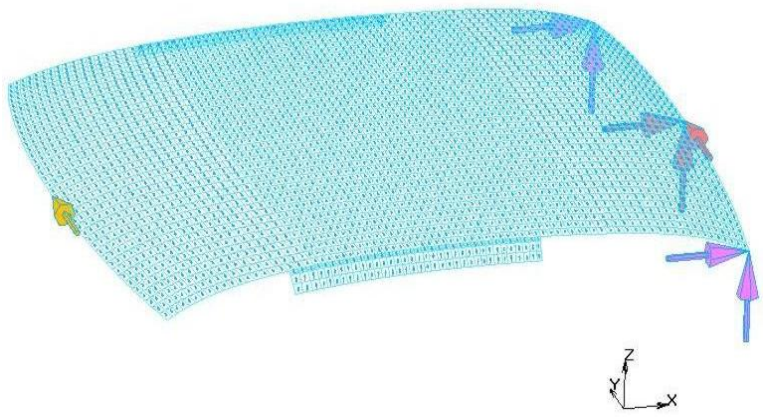

Figure 11: Finite element model of a composite roof, on which simple support boundary conditions are applied.

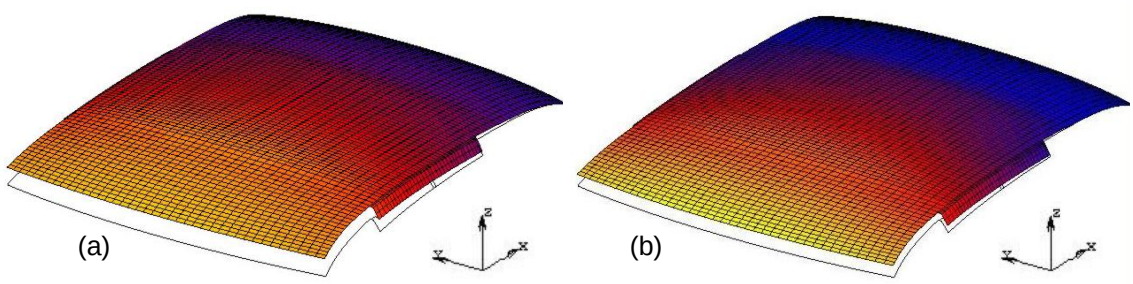

Figure 12: (a) Open mould (freely cured) and (b) closed mould symmetrically-laminated roof deformed upon removal from the mould at the end of the curing.

It can be seen that the overall deformation of the freely cured roof is larger than that of the closed mould roof. This is in agreement with the experimentally observed deformations of the square laminates, see Figure 5, which is attributed to the partial relaxation of the curing stresses in the mould. Furthermore, on the surface of the freely cured roof a concavity is obtained, which is not seen on the closed mould roof. The significant deformations obtained here are due to the curing shrinkage of the matrix resin before cooling, which cannot be avoided even for the closed mould products.

Conclusions

The curing-induced deformation of laminated car body panels is modeled by taking the orthotropic viscoelastic behavior of its laminas into account. The orthotropic properties of the lamina are obtained through the micro-mechanical analysis, by using the newly developed cure-dependent viscoelastic model for the resin. An experimental study on the curing deformation of asymmetric [90/0] laminates is perform to verify the model. The cylindrical shape of the cured laminates and the higher curvature of the freely curing laminate are very well predicted. Further, it is concluded that the curing stresses induce significant deformations in the composite panels which cannot be avoided even if the symmetric laminates are cured in a closed mould. The initial curvatures and bends of the panel in the mould affects its final deformed shape. Also, the curing stresses have a viscoelastic nature which may not be modeled by using the available elastic models.

References

1. White, S.R., Hahn, H.T., “Process Modeling of Composite Materials: Residual Stress Development during Cure. Part I. Model Formulation”, Journal of Composite Materials, 1992; 26(16): 2402-2422.
2. Kiasat, M.S., Ernst, L.J., Marissen, R., “Curing stresses in matrix resins containing filler and low profile additives”, Proc. 12th European Conference on Composite Materials (ECCM12), 2006, Biarritz, France.
3. Tseng, S.C., Osswald, T.A., “Predicting Shrinkage and Warpage of Thin Compression Molded Fiber Reinforced Thermoset Parts”, SAMPE Quarterly, 1993; 24(4): 40-48.
4. Bogetti, T.A., Gillespie, J.W., “Process-Induced Stress and Deformation in Thick-Section Thermoset Composite Laminates”, Journal of Composite Materials, 1992; 26(5): 626-660.
5. Wiersma, H.W., Peeters, L.J.B., Akkerman, R., “Prediction of Springforward in Continuous-Fibre/Polymer L-Shaped Pars”, Composites Part A, 1998; 29A: 1333-1342.
6. Hyer, M.W., “The Room-Temperature Shapes of Four-Layer Unsymmetric Cross-Ply Laminates”, Journal of Composite Materials, 1982; 16: 318-340.
7. Capehart, T.W., Muhammad, N., Kia, H.G., “Compensating Thermoset Composite Panel Deformation using Corrective Molding”, Journal of Composite Materials, 2007; 41(14): 1675-1701.
8. Kiasat, M.S., “Curing Shrinkage and Residual Stresses in Viscoelastic Thermosetting Resins and Composites”, Ph.D. thesis, 2000, Delft University of Technology, Delft, the Netherlands.